IEEE Access
Multidisciplinary ⋮ Rapid Review ⋮ Open Access Journal

Received 26 February 2024, accepted 1 April 2024, date of publication 18 April 2024, date of current version 6 May 2024.

Digital Object Identifier 10.1109/ACCESS.2024.3391052

RESEARCH ARTICLE

Image Segmentation Using Bias Correction Active Contours

HAMZA ZIA[1], SHAFIULLAH SOOMRO[2], AND KWANG NAM CHOI[1]
[1]Department of Computer Science and Engineering, Chung-Ang University, Seoul 06974, South Korea
[2]Department of Computer Science and Media Technology, Linnaeus University, 3016 Växjö, Sweden

Corresponding author: Kwang Nam Choi (knchoi@cau.ac.kr)

This work was supported in part by the Chung-Ang University Young Scientist Scholarship, in 2022; and in part by the High Performance Computing (HPC) Support Project funded by the Ministry of Science and ICT and National IT Industry Promotion Agency (NIPA).

ABSTRACT Deep learning-based image segmentation methods require densely annotated and massive datasets to produce effective results. On the other hand, active contours-based methods are excellent alternatives to the situation, producing acceptable segmentation results. Earlier active contour models, including local and global region information, struggle with their limitations, such as spurious contours appearing in inhomogeneous images. Bias correction is utilized to solve the bias field's energy, considering the intensity inhomogeneity and the level set functions that suggest an image domain division. In our approach, we combine the advantages of local and global information in the image level set function, resulting in a combined energy function that aids in the efficient evolution of contours on images and can judge the relevance of the item and its surroundings. The proposed model computes data force by extracting local information from an in-homogeneous image using image-fitting energy and then computing all pixel values simultaneously. Objects with high differences between grey levels or more in-homogeneity can be segmented. The outcome demonstrates that our method is more dependable and computationally efficient than previous methods.

INDEX TERMS Non-uniform intensity segmentation, distance adjustment term, active contour model, gradient approach, adaptive function.

I. INTRODUCTION

Image segmentation is essential in many applications, including machine learning, computer vision, and image analysis. The aim of segmentation is to distinguish the region of interest from the rest of the image for further applications. However, several methods devised for this task follow supervised and unsupervised streams of image processing and computer vision fields. The active contour model, belonging to the unsupervised techniques category of image segmentation models, has been a notable and commonly used approach for over two decades. The active contour model, often known as the snake model, uses a deformable contour that moves and adapts to object boundaries within an image repeatedly [2]. This contour is governed by an energy functional, which aims to minimize the energy cost of deformation. Active contours are computer-generated synthetic curves that move under the influence of two opposite forces: internal and external. Depending on the formulation of active contour models, they are broadly classified into edge-based and region-based, with their own limitations and strengths.

Edge-based active contour models detect object edges using gradient information. These models find regions with substantial variations in pixel intensity, which frequently correlate to object borders, by exploiting picture gradient coefficients [3]. While edge-based active contour is helpful in some situations, it is sensitive to initial contour placements and struggles to capture regions with weak or unclear boundaries. Furthermore, image noise can considerably influence the quality of gradient-based edge identification, resulting in compromised segmentation results [3], [4].

Region-based active contour models, on the other hand, adopt a different approach by using global image region infor-

The associate editor coordinating the review of this manuscript and approving it for publication was Yizhang Jiang.

mation rather than depending on gradients. The Mumford-Shah (M-S) [1] model-based C-V model employs the global intensity difference between the inner and outer regions of the contour's average intensities to drive the segmentation process is a prominent region-based active contour model. This region-based method is less susceptible to initial contour placement and works better with images with hazy edge points [5], [32]. Despite advances in both edge-based and region-based active contour models, researchers have discovered some drawbacks that restrict their effectiveness in real-world applications [35], [36]. These problems include the difficulty of dealing with images with non-uniform intensity distributions, the requirement for enhanced initialization resilience, and the necessity for more efficient segmentation approaches are among these problems.

We introduce an innovative approach aimed at overcoming the current limitations of image segmentation as addressed by active contour models. Our technique incorporates several key components, all working together to enhance the precision and effectiveness of the segmentation process.

To begin with, we introduce a novel distance adjustment term that dynamically modifies the step size of the current contour. This dynamic adjustment enables more accurate segmentation by precisely tracing object boundaries while minimizing excessive computational costs. In our quest to improve segmentation outcomes, we propose the incorporation of a length term. This term effectively filters out inefficient shapes, streamlining the segmentation process and leading to clearer and more meaningful results by eliminating superfluous forms. Furthermore, we leverage the gradient technique to enhance the total energy function, ensuring that the active contour efficiently converges towards the ideal segmentation results. Lastly, we introduce a localized image-fitting strategy based on a unique convolution kernel function tailored to address the challenge of non-uniform intensity segmentation. This localized approach adapts to regional image attributes, resulting in more dependable and precise segmentation outcomes, even in scenarios with varying intensity distributions. We show considerable gains in initialization robustness, efficiency, and segmentation accuracy compared to previous region-based models. Our methodology combines novel ideas and approaches, opening the way for more accurate and dependable picture segmentation in various real-world applications. Following are the specific contributions that our method offers.

- **Introduction of Dynamic Distance Adjustment Term:** We introduce a novel distance adjustment term that dynamically alters the step size of the active contour. This innovation enhances the accuracy and precision of segmentation by providing better control over the contour's movement.
- **Reduction of Redundancy with Length Term:** To eliminate redundant shapes and improve segmentation results, we propose the inclusion of a length term. This term effectively filters out unnecessary contours, resulting in more concise and relevant segmentation outcomes.
- **Optimizing Segmentation with Gradient Technique:** We employ the gradient technique to maximize the total energy function. This optimization leads to rapid convergence towards ideal segmentation results, enhancing efficiency in the process.
- **Local Image Fitting Strategy:** We introduce a localized image fitting strategy that relies on a specific convolution kernel function. This approach effectively addresses non-uniform intensity segmentation challenges, producing more reliable and accurate segmentation results. Additionally, it enhances initialization robustness, efficiency, and segmentation accuracy compared to previous region-based models.
- **Integration of Innovative Approaches:** Our work represents an integration of novel ideas and techniques aimed at enhancing the capabilities of the active contour model and image segmentation methods. These improvements are valuable for a wide range of real-world applications.

The remainder of this manuscript is organized as follows. Section II briefly presents the previous work. The proposed work is explained in Section III, whereas Section IV demonstrates the experiments and results. Finally, we conclude our research in Section V.

II. RELATED WORK

There are many region-based active contour models for image segmentation. This section briefly summarises related work as per the literature in the following subsections.

A. CHAN VESE MODEL

The Chan-Vese (CV) model stands as a prominent image segmentation methodology, originally conceived as a region-based approach adept at delineating objects within images characterized by indistinct borders and diminished gradient values [3]. Notably, it represents a robust and versatile solution for the segmentation of a wide spectrum of images, including those that have historically presented formidable challenges for conventional segmentation methods, such as thresholding [3].

At its core, the CV algorithm operates by minimizing an energy functional. This functional encompasses weighted terms, including the summation of intensity differences from the mean value in regions external to the segmented area, the summation of differences from the mean within the segmented area, and an associated term dependent on the length of boundaries within the subdivided regions [3]. The model traces its lineage to the Mumford-Shah (M-S) model and has found significant application within the realm of imaging, particularly in domains characterized by authentic and complex imagery, such as neuroimaging, magnetic resonance imaging (MRI), and cardiac imaging,

among others [2], [3], [29].

$$E_{cv}(C, c1, c2) = \mu \,\text{len}(C) + \lambda_1 \int_{\text{outside}}^{\text{outside}} C(I(x) - c1)^2 \, dx + \lambda_2 \int_{\text{inside}}^{\text{inside}} C(I(x) - c2)^2 \, dx \tag{1}$$

In the provided formulation, the parameters lambda1 and lambda2 are user-defined, while the constants c1 and c2, as specified in the formula, play a pivotal role in the estimation of object intensities situated within and outside the contour, as indicated by the relevant reference [2]. The contour curves are subject to a decremental energy zeroing function, with the Uhler equation being employed to facilitate a reduction in the gradient. Furthermore, an energy reduction process to achieve a zero-level adjustment function is applied to the curve denoted as c. Utilizing the diminishing energy zeroing function in the context of contour curves is a central component of the methodology, as elucidated by the reference in question.

$$\begin{aligned} E^{CV}(\phi, c1, c2) = v \int_{\sigma} H_\epsilon(\phi) \, dx \\ + \mu \int \sigma_\epsilon(\phi)[\delta\phi] \, dx \\ + \lambda_1 \int_{\text{outside}}^{\text{outside}} C(I(x)c1) H_\epsilon \, dx \\ + \lambda_2 \int_{\text{inside}}^{\text{inside}} (C)(I(x)c2) H_\epsilon^d x \end{aligned} \tag{2}$$

where H_ϵ is the Heaviside function with ϵ constanct.

The following equation can define the Heaviside function.

$$H_\epsilon(x) = \frac{1}{2}\left[1 + \frac{2}{\pi} \arctan\left(\frac{y}{\epsilon}\right)\right] \tag{3}$$

The Heaviside function is also known as the unit step function, returning a zero value for $x < 0$. After calculating the variations and determining the values of c_1 and c_2, the available minimization formula is:

$$\begin{aligned} C_1, \sigma_\epsilon &= \frac{\int H_\epsilon(\phi) I(y) dy}{H'_\omega \int H_\epsilon(\phi) I(y) dy}, \\ C_2, \sigma_\epsilon &= \frac{\int H_\epsilon(\phi) I(y) dy}{H'_\omega \int H_\epsilon(\phi) I(x) dy}. \end{aligned} \tag{4}$$

The C-V model assumes that the target and background of an image are statistically homogeneous [34]. However, when the image intensities exhibit significant variation, it can lead to improved segmentation performance.

$$\phi(X) > 0 \quad \text{if} \quad x \in \text{In}(C) \tag{5}$$

$$\phi(X) = 0 \quad \text{if} \quad x \in \text{on}(C) \tag{6}$$

$$\phi(X) > 0 \quad \text{if} \quad x \in \text{out}(C) \tag{7}$$

B. LBF

Local binary fitting is employed to extract local information within images, which can pertain to identification or recognition purposes. In certain cases, images characterized by grey values or grayscale imagery may not yield discernible results or may pose challenges in obtaining satisfactory outcomes [21]. The Local Binary Fitting (LBF) model is specifically designed to address such issues more efficiently. By employing function approximation to estimate pixel values, the energy contour within the energy function is initially adjusted inward and subsequently shifted outward to obtain the desired result. LBF serves as a valuable tool for addressing image inhomogeneities.

$$\begin{aligned} \epsilon_x(Q, f_1(a), f_2(b)) = \\ \lambda_1 \int_{\text{in}(C)} K_\sigma(a-b)[I(b) - f_1(a)]^2 \, dy + \\ \lambda_2 \int_{\text{out}(C)} K_\sigma(a-b)[I(b) - f_1(a)]^2 \, dy \end{aligned} \tag{8}$$

In the context of image processing, the input domain comprises image data, and Gaussian kernel function values are represented as $f_1(a)$ and $f_2(b)$, which are two distinct functions employed for fitting the contour of the image. When an object is situated at the boundary of the image, this reduces local energy, causing a shift both inside and outside the image boundaries.

$$\epsilon(C, f_1, f_2) = \int_\omega \epsilon_x(C, f(a), f2(b)) \, dx \tag{9}$$

$$\begin{aligned} \epsilon(\phi, f_1, f_2) &= \int_\omega \epsilon_x(\phi, f(a), f2(b)) \\ &= \lambda_1 \int \left[\int K_\sigma(a-b)[I(b) - f_1(a)]\right]^2 \\ &\quad H(\phi(a)) \, dy \; dx \\ &\quad + \lambda_2 \int \left[\int K_\sigma(b-a)[I(a) - f_2(b)]\right]^2 \\ &\quad [1 - H(\phi(b))] \, dy \; dx \end{aligned} \tag{10}$$

$$f_1(x) = \frac{K_\sigma(a) * [H_\epsilon(\phi(b)) I(a)]}{K_\sigma(b)} * H_\epsilon(\phi(a)) \tag{11}$$

$$f_2(x) = \frac{K_\sigma(b) * [H_\epsilon(\phi(a)) I(b)]}{K_\sigma(a)} * H_\epsilon(\phi(a)) \tag{12}$$

For the representation of the LBF model:

$$\begin{aligned} E_{\text{lbf}}(\phi, f_1, f_2) = \sum_{\infty} \lambda_i \\ \int_\omega \int_\omega k_r(a-b)(I(b) - f_i(a))^2 H_i(\phi(a)) \, dx \end{aligned} \tag{13}$$

The presented formula incorporates a Gaussian kernel characterized by a specific standard deviation, including two smoothing functions denoted as h_1 and h_2. These smoothing functions are instrumental in approximating local intensity and contour values denoted as C [8], [21]. The selection of an appropriate standard deviation assumes paramount importance in practical applications. Careful consideration is warranted during this selection process, as an excessively low standard deviation may yield unsatisfactory results while

opting for excessively high values can result in a considerable computational burden. It is imperative to acknowledge that the computational demands of local binary fitting models are notably high, necessitating numerous iterations for each computation.

C. DRLSE

This deletion regulates the evolution of the level set and eliminates the need for re-initialization, so no numerical errors occur [33]. This is how Distance controls level set evolution and allows for efficient initialization. Distance regularization level set evolution increases the number of iterations and requires more time steps, which improves model accuracy and is applicable to edge-based models [16], [30].This is how Distance controls level set evolution and allows for efficient initialization.

D. LIF

The local image fitting (LIF)model exhibits the capability to segment non-uniform images effectively. An innovative Gaussian-based model has been introduced to fine-tune the level set information, rendering re-initialization unnecessary, which is not only computationally expensive but also eliminates the need for it [21]. It is essential to note that while re-initialization has been eliminated in this context, its requirement persists in certain situations [5]. The efficiency of this model notably surpasses that of the LBF model [21].

The level set function is formulated as

$$E_{lif} = 12 \int_{\omega} |I(a) - I_{LFI}(a)|^2 \, dx \tag{14}$$

For the calculation of local features in the image, the following equation is used:

$$I_{lif}(a) = m1(a)H_{\epsilon}(\phi) + m2(a)(1 - H_{\epsilon}(\phi)) \tag{15}$$

Here, in the equations for H1 and H2, both are local mean intensities calculated as:

$$H_1 = \text{mean}(I(a)|\phi(a) < 0, a \in \omega \cap \text{WU}(a)) \tag{16}$$

$$H_2 = \text{mean}(I(a)|\phi(a) > 0, a \in \omega \cap \text{WU}(a)) \tag{17}$$

$$\epsilon_x(L, f_1(a), f_2(a)) = \lambda_1 \int_{\text{in}(C)} K_\sigma(a-b)[I(b) - f_1(a)]^2 \, dy + \lambda_2 \int_{\text{out}(C)} K_\sigma(a-b)[I(b) - f_1(a)]^2 \, dy \tag{18}$$

Now, for the input domain of the image and having Gaussian kernel function values, $f_1(x)$ and $f_2(x)$ are two functions used for fitting the image contour. When the object is in the boundary of the image, it will reduce the local energy inside and outside of the image.

$$\epsilon(C, f_1, f_2) = \int_{\omega} \epsilon_x(C, f(a), f_2(a)) \, dx \tag{19}$$

$$\epsilon(\phi, f_1, f_2) = \int_{\omega} \epsilon_x(\phi, f(a), f_2(a)) + \lambda_1 \int \left[\int U_\sigma(a-b)[I(b) - f_1(a)] \right]^2 H(\phi(y)) \, db \, da + \lambda_2 \int \left[\int U_\sigma(b-a)[I(b) - f_2(a)] \right]^2 [1 - H(\phi(y))] \, db \, da \tag{20}$$

$$f_1(x) = \frac{U_\sigma(a)[H_\epsilon(\phi(a))I(a)]}{K_\sigma(a)} H_\epsilon(\phi(a)) \tag{21}$$

$$f_2(b) = \frac{U_\sigma(a)[H_\epsilon(\phi(b))I(a)]}{K_\sigma(b)} H_\epsilon(\phi(b)) \tag{22}$$

E. LSACM

For each local region, the algorithm generates a bias field, a level-set function, and a statistical energy function, all containing successive approximations to the true signal associated with the respective object. The proposed Active Contour Model (ACM) demonstrates its versatility by simultaneously addressing both segmentation and bias correction. It excels particularly in initialising the level set function, allowing for seamless automatic application [17]. Experimental results obtained from synthetic and real photographs affirm the superiority of the proposed approach when compared to current representative methods. The strength of the ACM lies in its adeptness at initializing the level set function and facilitating automatic application.

F. LPF

The local pre-fitting energy plays a crucial role in the determination of two pre-fitting parameters, achieved by regionally averaging the image intensity prior to curve unrolling. Empirical observations validate the resilience of the proposed approach to different initializations, which is a noteworthy advantage. The utilization of a small constant function as the initial level adjustment function further contributes to efficient segmentation, thus saving valuable computational resources [15]. A comparative assessment against other models reliant on local adjustments underscores the merits of the LPF (Local Pre-Fitting) method. This approach can be effectively applied to various local fitting-based models, bolstering the robustness of initial contours while simultaneously reducing computational overhead [5].

$$Ex(c) = outside(C) \cap x|I(y) - fs(x)|^2 dy + inside(c) \cap x|I(y) - f1(x)|^2 dy \tag{23}$$

Below, the functions F and ω can be directly calculated, which are divided by a line and represented by C at

the given point.

$$E_x(f) = \int (x-y)[I(y) - f_s(x)]^2 dy + \int K_\sigma(x-y)[I(y) - f_1(x)]^2 dy \quad (24)$$

Energy can be minimized at the given point below. A Gaussian function is employed as a fitting-based model, but it can be replaced by the local omega ω_x due to its localization property. The curves will remain at the boundary even when the LPF (Local Pre-Fitting) is minimized, with regions farther away from the boundary containing more curves.

$$E^{LPF}(f) = \int_\omega \left(\int_{outside} K_\sigma(x-y)[I(y) - f_s(x)]^2 dy \right) + \int_\omega \left(\int_{inside} K_\omega(x-y)[I(y) - f_1(x)]^2 dy \right) dx \quad (25)$$

$$E^{LPF}(\phi) = \int_\omega \left(\int_\omega K_\sigma(x-y)[I(y) - f_s(x)]^2 H_\epsilon(\phi(y)dy) \right) dx + \int \left(\int_\omega K_\omega(x-y)[I(y) - f_1(x)]^2 (1 - H_\epsilon(\phi(y)dy) dx \right) \quad (26)$$

III. PROPOSED METHOD

Through the incorporation of both local and global contextual information within an active contour model, our proposed methodology introduces a novel approach to image segmentation. This approach not only aims to expedite the computational process but also strives to yield highly accurate results.

In the initial stages, we leverage the intrinsic local characteristics of the image to enhance the segmentation process. This involves the extraction of comprehensive local information through techniques such as binary analysis and local image fitting. This approach enables us to capture fine-grained features within the image, thereby enhancing the precision of segmentation. Moreover, the integration of binary information allows for a more efficient distinction between foreground and background regions, expediting the overall segmentation procedure. Fig. 8 is the graphical abstract of the proposed methodology.

A. INCORPORATION OF INFORMATION AT THE PIXEL LEVEL (LOCAL WEIGHT FUNCTION)

We amalgamate pertinent energy terms into a hybrid energy function after capturing both pixel-level components and global image features.

The pixel-level components take into consideration the attributes of individual pixels and comprise two key terms: the pixel-level components term (referred to as the ''local term'') and the pixel-level gradient components term (referred to as the ''local gradient term'').

The pixel-level components term quantifies the dissimilarity between the pixel intensity $I(x, y)$ and the locally computed mean intensity. It is defined as:

$$E_{\mathrm{L}}(x, y) = \left| Q(x, y) - \frac{1}{M} \sum_{i=1}^{M} Q(y_i, x_i) \right|^2 \quad (27)$$

Here, M represents the number of neighboring pixels considered when calculating the local mean intensity.

The pixel-level gradient term assesses the variations in image gradients within a small neighborhood:

$$E_{\mathrm{grad}}(x, y) = |\nabla I(x, y)|^2 \quad (28)$$

In addition, we introduce global terms to capture the broader image context. The global intensity term accounts for the overall intensity distribution within the image, constraining pixel intensity differences relative to the global mean intensity:

$$E_{\mathrm{global}}(x, y) = \left| Q(x, y) - \frac{1}{M} \sum_{j=1}^{M} I(x_j, y_j) \right|^2 \quad (29)$$

To promote contour smoothness during evolution, we incorporate a regularization term. The level set function, aimed at minimizing fluctuations in this context, is described as:

$$E_{\mathrm{reg}}(x, y) = |\nabla \phi(x, y)|^2 \quad (30)$$

The hybrid energy function is constructed as the sum of the individual energy components, with local and global information contributions weighted by w_{local} and w_{global} respectively:

$$E_{\mathrm{hybrid}}(x, y) = w_{\mathrm{local}} \cdot (E_{\mathrm{L}}(x, y) + E_{\mathrm{grad}}(x, y)) + w_{\mathrm{global}} \cdot (E_{\mathrm{global}}(x, y) + E_{\mathrm{reg}}(x, y)) \quad (31)$$

The hybrid energy function seamlessly incorporates both local and global information, facilitating a comprehensive image analysis that ensures accurate segmentation.

In pursuit of correct segmentation, our approach leverages gradient descent flow in tandem with the Spatial Prior Function (SPF). The gradient descent flow, as it minimizes the energy function, guides the contour towards an optimal segmentation solution.

The SPF, as described in [17], embodies spatial prior knowledge and plays a pivotal role in steering contour evolution by imposing constraints rooted in spatial correlations.

Through the fusion of gradient descent flow and the SPF, our model achieves superior contour stability, enhanced convergence, and precise boundary detection, making it a robust choice for image segmentation.

B. EVOLUTION OF CONTOURS AND MULTIFUNCTIONAL ENERGY FUNCTION

We elucidate the intricacies of the hybrid energy function and its influence on contour evolution in our proposed model for image segmentation in this paragraph. Our methodology yields precise and reliable segmentation results

by amalgamating local and global information, utilizing gradient descent flow, and incorporating the Signed Pressure Force (SPF).

Fusion of Local and Global Information:

We consolidate relevant energy terms into the hybrid energy function to encompass both local and global image features.

The local information component comprises the local intensity term and the local gradient term, both pertaining to pixel-level attributes. The local intensity term, denoted as $E_L(x, y)$, quantifies the dissimilarity between the local mean intensity and the pixel intensity $I(x, y)$ and is defined as:

$$E_{\mathrm{L}}(x, y) = \left| Q(x, y) - \frac{1}{M} \sum_{i=1}^{M} I(x_i, y_i) \right|^2 \tag{32}$$

Here, M represents the number of neighboring pixels used to calculate the local mean intensity, and $I(x_i, y_i)$ signifies the pixel value at coordinates (x_i, y_i) in the original image. $Q(x, y)$ represents the pixel value at coordinates (x, y) in the segmented image. This equation quantifies the local information necessary for precise segmentation by comparing the segmented pixel value to the average intensity of the relevant region in the original image.

The local gradient term, $E_{\mathrm{grad}}(x, y)$, quantifies variations in image gradients within a local neighborhood and is defined as:

$$E_{\mathrm{grad}}(x, y) = |\nabla Q(x, y)|^2 \tag{33}$$

Here, $\nabla Q(x, y)$ represents the gradient of the pixel value at coordinates (x, y) in the segmented image. This term provides information about the local image structure by quantifying gradient variations within the segmented region, incorporating edge and boundary information essential for precise segmentation.

Additionally, we introduce the regularization term $E_{\mathrm{reg}}(x, y)$ to impose spatial constraints and promote smoothness in contour evolution. It is defined as:

$$E_{\mathrm{reg}}(x, y) = |\nabla \phi(x, y)|^2 \tag{34}$$

This term minimizes variations in the level set function, contributing to contour stability.

The hybrid energy function integrates both local and global information, allowing for a more comprehensive image analysis to achieve accurate segmentation. It is defined as follows:

$$\begin{aligned} E_{\mathrm{hybrid}}(x, y) = {} & w_{\mathrm{L}} \cdot (E_{\mathrm{L}}(x, y) + E_{\mathrm{grad}}(x, y)) \\ & + w_{\mathrm{G}} \cdot (E_{\mathrm{global}}(x, y) + E_{\mathrm{reg}}(x, y)) \end{aligned} \tag{35}$$

where w_{L} and w_{G} are weighting variables governing the influence of local and global components, respectively.

Gradient Descent Flow:

By minimizing the energy function, gradient descent flow propels the contour towards the optimal segmentation solution. It iteratively updates the contour using gradients of the energy function and is expressed as:

$$\frac{\partial \phi}{\partial t} = -\frac{1}{|\nabla \phi|} \nabla \cdot \left(\alpha \nabla E_{\mathrm{hybrid}} \right) \tag{36}$$

Signed Pressure Force (SPF): Integrating the signed pressure force in eq(36) is important because it contains the pressure force that will give the internal force operating within the contour from the stability mechanism, and the outside compelling factor is reinforced by signed pressure force, or F_P.

The following modified formulation may be gained by incorporating the signed pressure building block which manages the enhancement of the outline

$$\frac{\partial \phi}{\partial t} = -\frac{1}{|\nabla \phi|} \nabla \cdot (\alpha \nabla E_{\mathrm{hybrid}} + \mathbf{F}_P) \tag{37}$$

The most active part inside the shape is shown by the signed pressure force, F_P. Determined by the form or curvature of the contour, it is driven to the inner side and outer side.

Now that is important to carry out into the signed pressure force.

It is vital to take into account the SPF factor's connections to the various other vital factors. The SPF helps to maintain the contour's consistency and smoothness by protecting it from outside influences and preventing it from growing or shrinking.

The equation includes the gradient of the hybrid energy function $\delta_{E\,\mathrm{hybrid},which is key to controlling the contour motion}$

Hybrid energy gradient or $\delta_{E_{\mathrm{hybrid}}}$

E_L (Local Energy):

E_L captures local image information that affects contour movement. This is usually related to image properties such as edges, textures, or shifts in the intensity of certain areas. The word $|\nabla \phi|$ in the denominator indicates the magnitude of the gradient of the contour function ϕ.

The direction and extent of the change in the energy environment is indicated by the slope of the hybrid energy function. The mechanism regulates contour growth using multiple energy sources.

E_grad (Gradient Energy):

The segment that contains the gradient-based energy, symbolized by $\alpha \Delta E_{\mathrm{grad}}$. In order to assist in boundary identification or capturing image edges, it controls the contour towards regions with extensive image gradients. The regularization energy, or E_{reg}, ensures that the contour is smooth and prevents it from fragmenting by applying regularization. It strikes a compromise between preserving the contour's smoothness to prevent unpredictable forms and adapting it to the image data (E_L). The Signed Pressure Force, commonly known as SPF, incorporates spatial prior knowledge and guides contour evolution by imposing additional constraints based on spatial correlations. It leverages prior knowledge about the image's spatial coherence to refine contour movement and is expressed as:

$$F_{\mathrm{SPF}} = \beta \cdot \mathrm{SPF}(\phi) \tag{38}$$

TABLE 1. CPU time and number of iterations required for segmentation for different active contour methods.

Method		Column 1	Column 2	Column 3
LIF [5]	CPU Time Iterations	12.34 60	6.52 100	10.23 100
WHRSPF [26]	CPU Time Iterations	8.23 60	4.23 40	6.23 100
DRLSF [33]	CPU Time Iterations	6.25 60	5.23 40	7.45 100
HLFRA [8]	CPU Time Iterations	4.11 60	3.22 40	5.23 100
Propsed	CPU Time Iteartions	1.32 60	0.923 40	2.33 100

Our model demonstrates superior contour stability, enhanced convergence, and precise boundary detection through the integration of gradient descent flow with SPF.

In our proposed model, the hybrid energy function, gradient descent flow, and SPF are seamlessly integrated, resulting in precise and reliable image segmentation. This approach effectively integrates local and global information, making it adaptable to various image characteristics. The weighting parameters w_{L} and w_{G} provide flexibility in emphasizing specific image aspects during segmentation. Additionally, the contour evolves toward an optimal solution while considering spatial constraints, thanks to the combination of gradient descent flow and SPF.

Through extensive experimentation and comparisons, we have demonstrated the effectiveness of our model in delivering improved segmentation outcomes, surpassing previous approaches in terms of accuracy and resilience. We also introduce the parameter λ_1 into the energy function to fine-tune the segmentation process, allowing for the adjustment of various variables in the energy functional to adapt segmentation based on specific image properties. This parameterized energy function is given by:

$$E_{\mathrm{T}}(x, y) = \lambda_1 \cdot E(x, y) \tag{39}$$

Additionally, we employ an epsilon value, denoted as ϵ, to reduce noise and ensure smoother segmentation output. This value helps reduce differences in pixel values between the center and nearby pixels, resulting in a noise-reduced modified energy function defined as follows:

$$E_{\mathrm{S}}(x, y) = \left| I(x, y) - \frac{1}{M} \sum_{i=1}^{M} I(x_i, y_i) \right|^2 + \epsilon \tag{40}$$

Our proposed method enhances image segmentation accuracy, resilience, and adaptability by combining parameter adjustments and noise reduction techniques. Extensive experiments and comparisons demonstrate the effectiveness of our approach across various image analysis applications.

IV. EXPERIMENTS AND RESULTS

We present a comprehensive examination of the results produced by our proposed image segmentation model in this section. The experiments were conducted on a machine equipped with a 7th generation Core i7 processor running at 2.7GHz, a GTX 960 GPU, 8GB of RAM, and Windows 10 with Matlab version 2018a. For our model, we employed a level set function with the following parameters: $\sigma = 5$, $\epsilon = 0.5$, $\delta t = 0.2$, $\mu = 4$, and $v = 0.01 \times 255 \times 255$. The α and λ values were fine-tuned to match the unique characteristics of each image, allowing for customization and achieving the desired segmentation results; see Figure 1, Figure 2, Figure 3, Figure 4 and Figure 5.

A. EVALUATION OF SEGMENTATION EFFECT ON INTENSITY INHOMOGENEOUS DATA:

We conducted experiments on a diverse set of images to assess the effectiveness of our model on different types of intensity inhomogeneous data. The results confirmed the efficacy of our approach, particularly in handling images with irregular black borders, which often posed challenges for conventional segmentation algorithms. Our model successfully identified and segmented objects with complex boundaries by employing the level set and energy function. To optimize the model's performance, we set the parameter values to $\lambda = 0$ and $\beta = 0.5$. Figure 5 presents the segmentation results for various parameter values, clearly illustrating the improvements over previous methods, especially for images with high levels of noise.

B. MODEL RESILIENCE WITH WEAK EDGES AND INHOMOGENEOUS IMAGES:

We evaluated the robustness of our model with respect to the initial contour placement on the image. A comprehensive experiment was conducted to assess its performance compared to other models such as WHRSPF [28] and DRLSE [8]. During the segmentation process, our model exhibited remarkable resilience and efficiency. Sensitivity to the initial contour was significantly reduced, resulting in more accurate edge detection and smoother regions within the image. Our model required fewer iterations to converge to the desired segmentation outcome, outperforming competing models that often struggled with weak edges and noisy images. Furthermore, our model achieved segmentation in significantly less time than previous methods, demonstrating its efficiency and computational advantages.

C. QUANTITATIVE COMPARISON:

We conducted an extensive comparison of the performance of our proposed model with several existing approaches, employing metrics such as Accuracy, Dice Index, and Sensitivity. These metrics provided insights into the correspondence between the selected regions and the ground truth of the images. The Accuracy metric quantified the proportion of true positive and true negative classifications, while the Dice Index measured the overlap between the designated regions and the actual image portions. Sensitivity assessed the model's ability to accurately identify specific regions of interest.

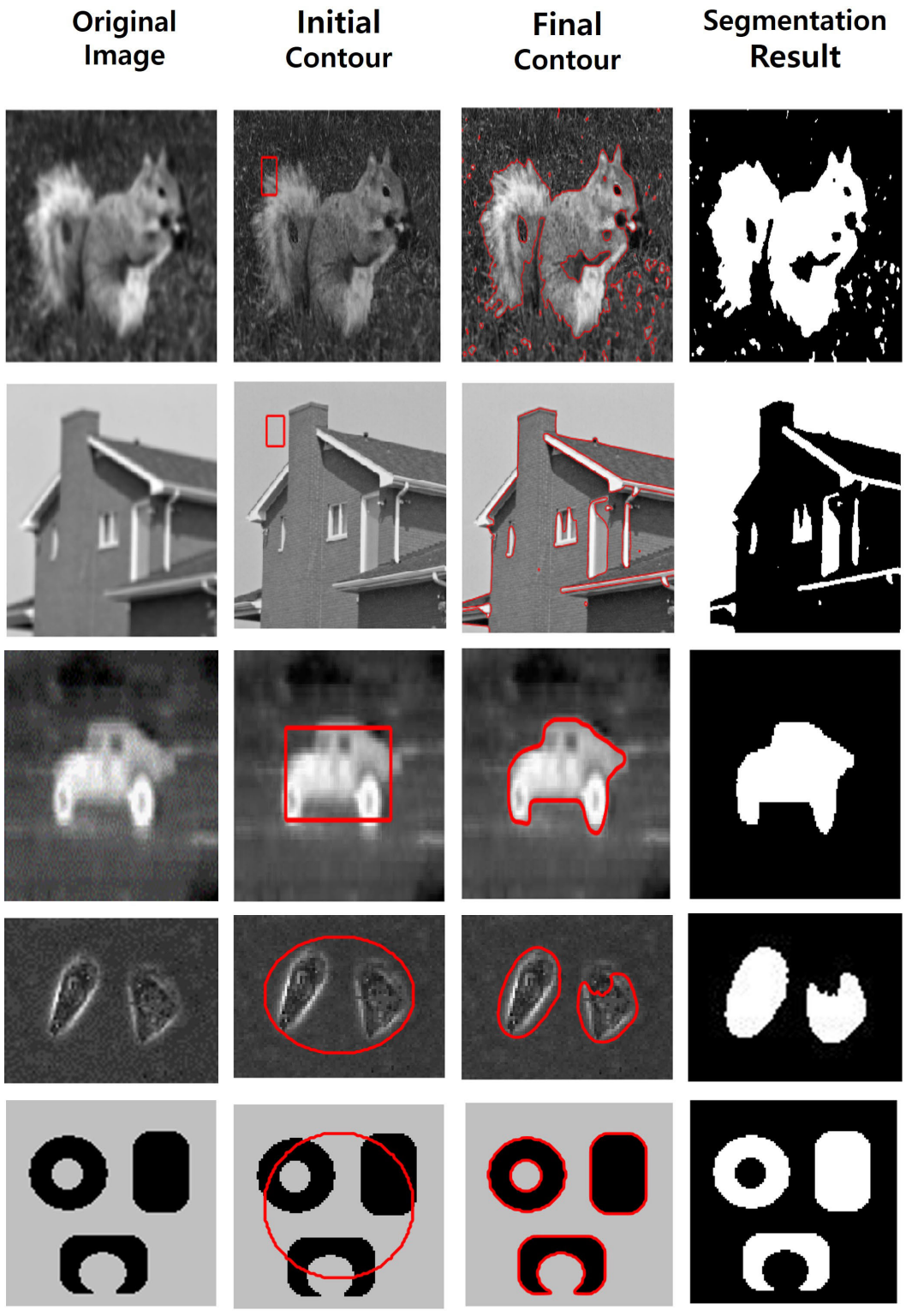

FIGURE 1. A series of images is presented, showcasing the segmentation results achieved by the proposed model.

we introduce the critical evaluation metrics utilized in our study, namely True Positive (**TP**), True Negative (**TN**), False Positive (**FP**), and False Negative (**FN**). These metrics play a pivotal role in assessing our proposed image segmentation model's performance. Furthermore, we present a quantitative evaluation of angiogram images, accompanied by a graphical representation of the average CPU time (in seconds) required for the segmentation of actual regions, the accurate exclusion of unsegmented areas, the identification of false regions, and the detection of undetected actual regions.

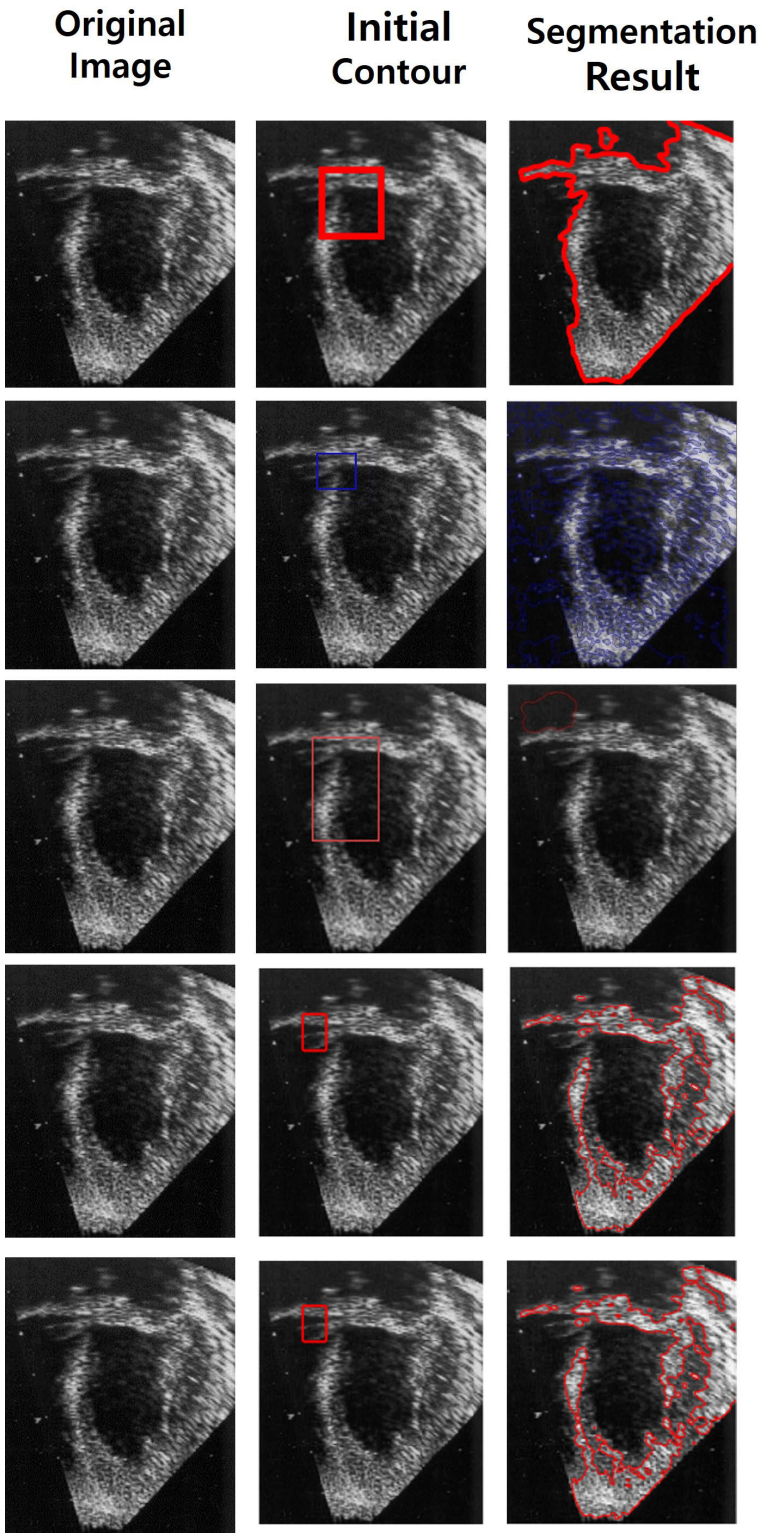

FIGURE 2. Segmentation results of various models including the proposed method: (Top Row) WHRSPF, (Second Row) DRLSE, (Third Row) LIF, (Fourth Row) HLFRA, (Fifth Row) proposed model.

This visual representation serves to underscore the efficiency and accuracy of our model in contrast to other established techniques. See Table 1 and Table 2 for tabular data of our evaluations.

Accuracy:

$$\text{Accuracy} = \frac{TP + TN}{TP + TN + FP + FN}$$

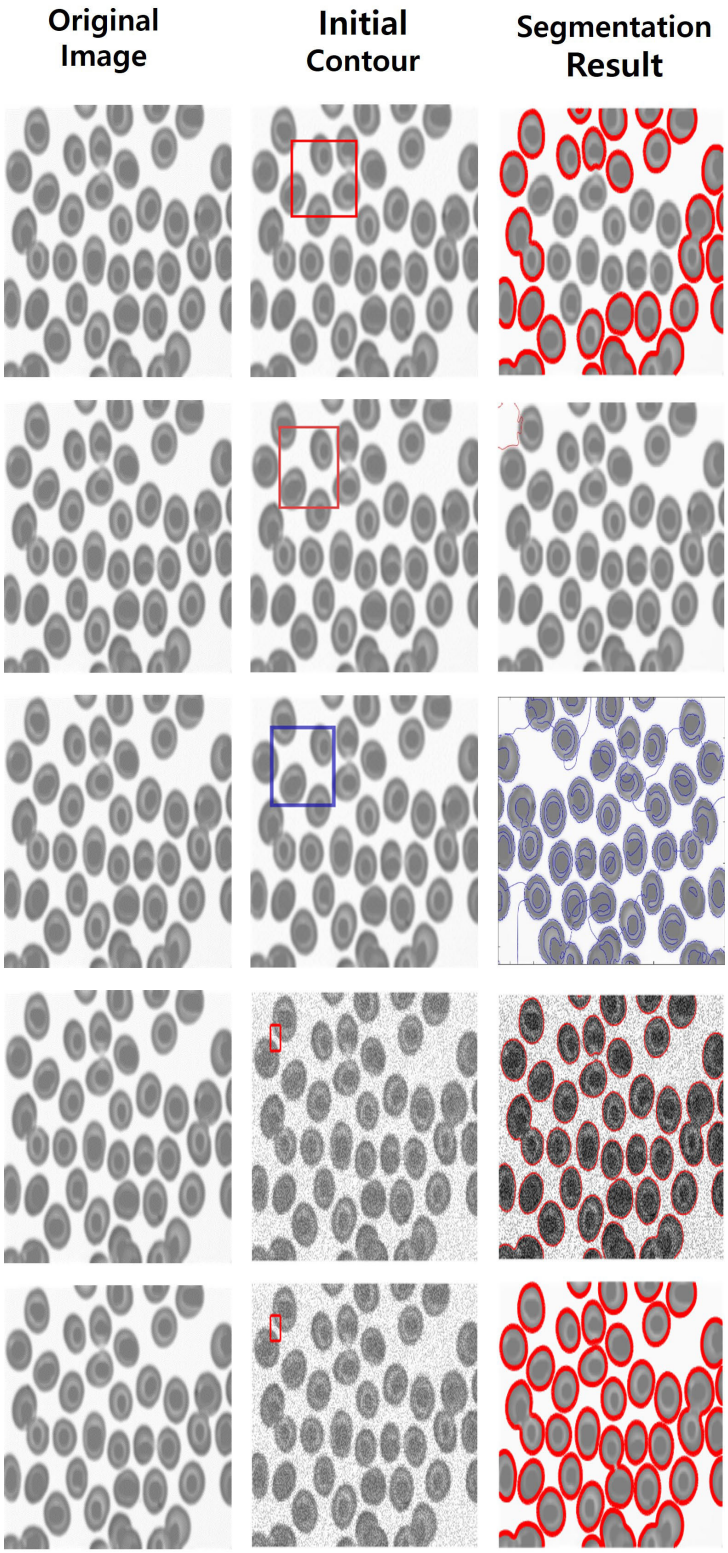

FIGURE 3. Segmentation results of various models including the proposed method: (Top Row) WHRSPF, (Second Row) DRLSE, (Third Row) LIF, (Fourth Row) HLFRA, (Fifth Row) proposed model.

Dice Index:

$$\text{Dice Index} = \frac{2 \times TP}{2 \times TP + FP + FN}$$

Sensitivity:

$$\text{Sensitivity} = \frac{TP}{TP + FN}$$

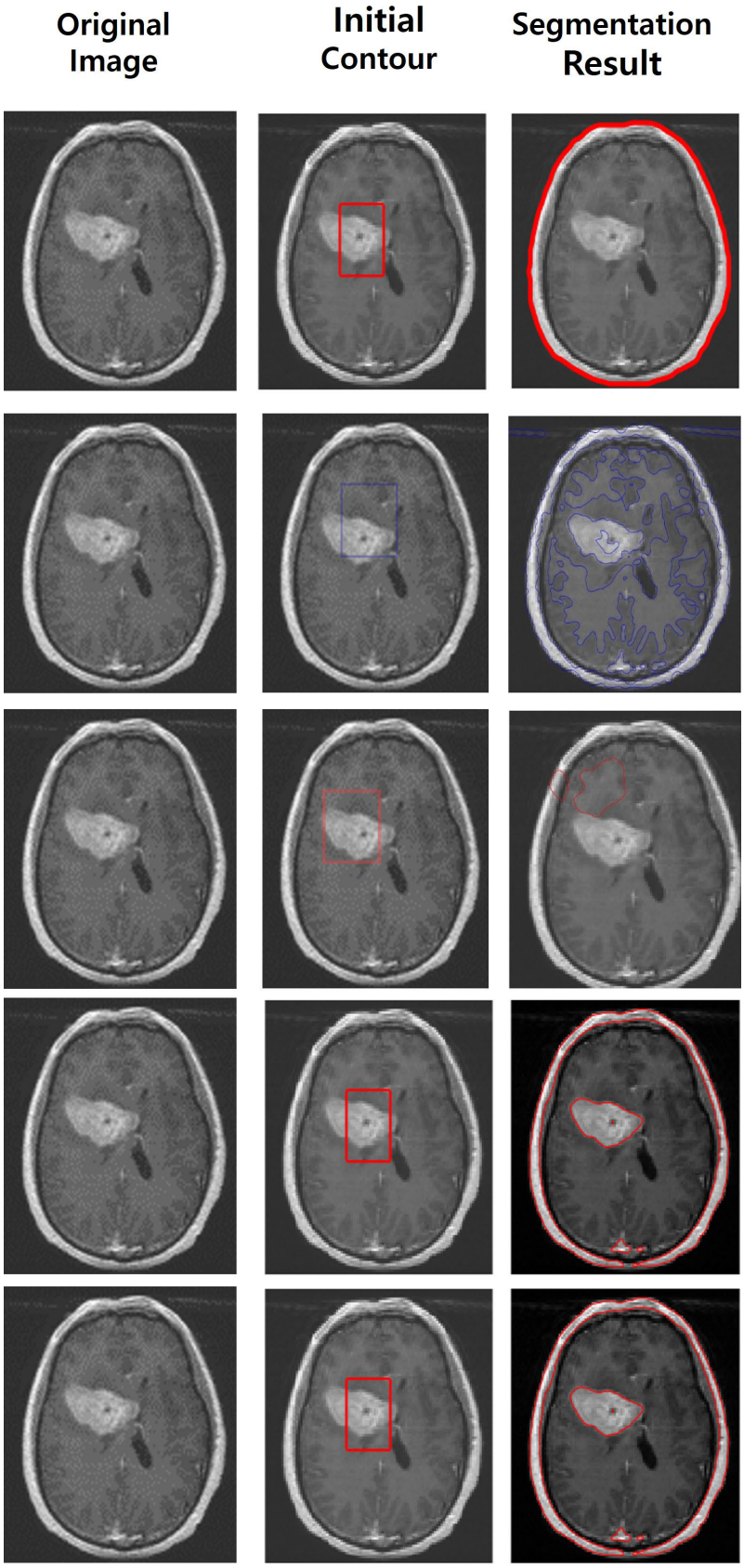

FIGURE 4. Segmentation results of various models including the proposed method: (Top Row) WHRSPF, (Second Row) DRLSE, (Third Row) LIF, (Fourth Row) HLFRA, (Fifth Row) proposed model.

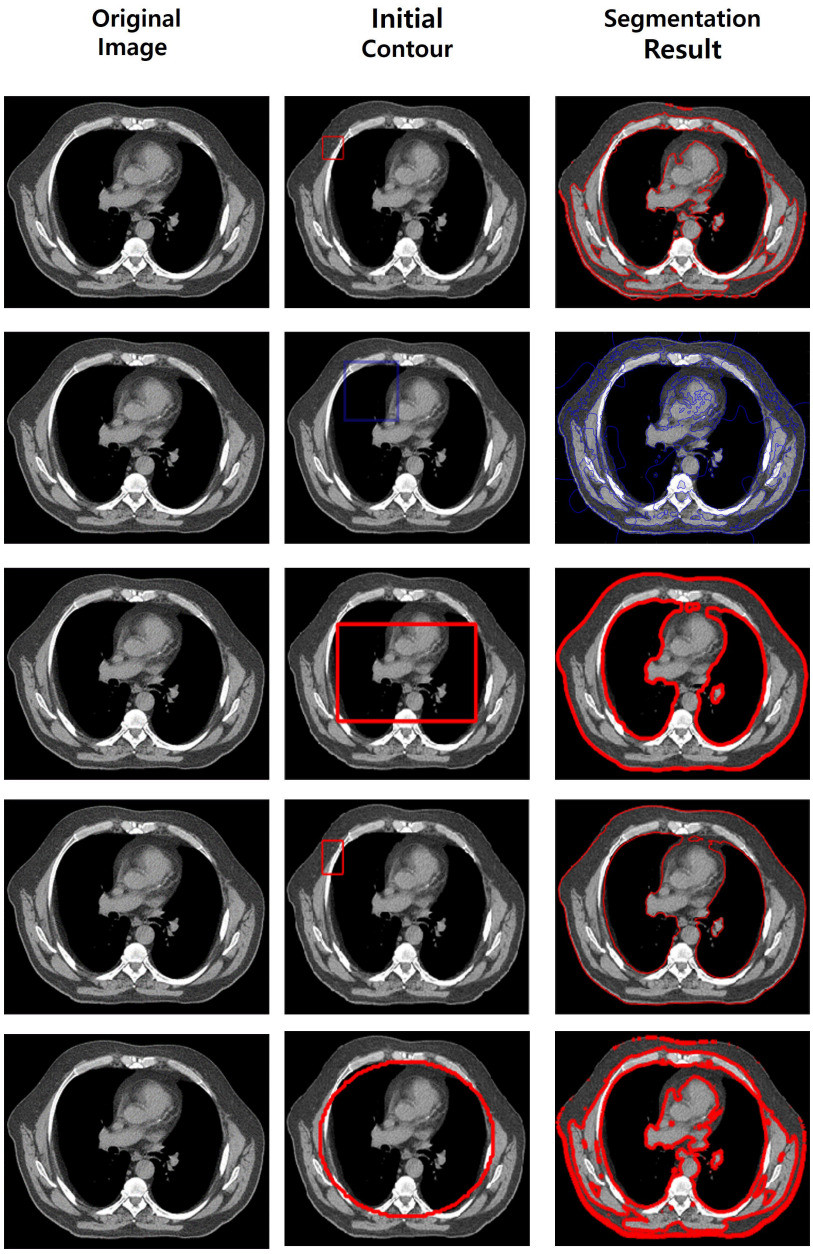

FIGURE 5. Segmentation results of various models including the proposed method: (Top Row) CV, (Second Row) LIF, (Third Row) GLFIF, (Fourth Row) HLFRA, (Fifth Row) proposed model.

TABLE 2. JS score evaluation of different image restoration methods.

Images	CV	GMAC	ICTM	WBHV	HLFRA	LBF	LIC	Ours
1	0.8029	0.7903	0.5420	0.0640	0.4437	0.0546	0.8091	0.9123
2	0.9496	0.9526	0.8652	0.7646	0.6787	0.1692	0.9513	0.9460
3	0.8040	0.8086	0.5428	0.1857	0.5634	0.0462	0.8123	0.9543
4	0.8606	0.8038	0.8417	0.4646	0.6731	0.0534	0.8766	0.9960
5	0.8108	0.7938	0.3198	0.0466	0.5490	0.0239	0.8254	0.9543
6	0.8537	0.8525	0.6776	0.3785	0.6620	0.1058	0.8679	0.9543
7	0.8207	0.8256	0.6760	0.1069	0.6619	0.0980	0.8304	0.9342
8	0.6872	0.7004	0.3521	0.0422	0.4260	0.0243	0.7093	0.9242
9	0.8358	0.8610	0.4184	0.0637	0.5561	0.0419	0.8576	0.9142
10	0.8201	0.8214	0.6223	0.0493	0.5503	0.0405	0.8244	0.9342
11	0.7190	0.7714	0.5497	0.1817	0.4527	0.1550	0.7425	0.9842

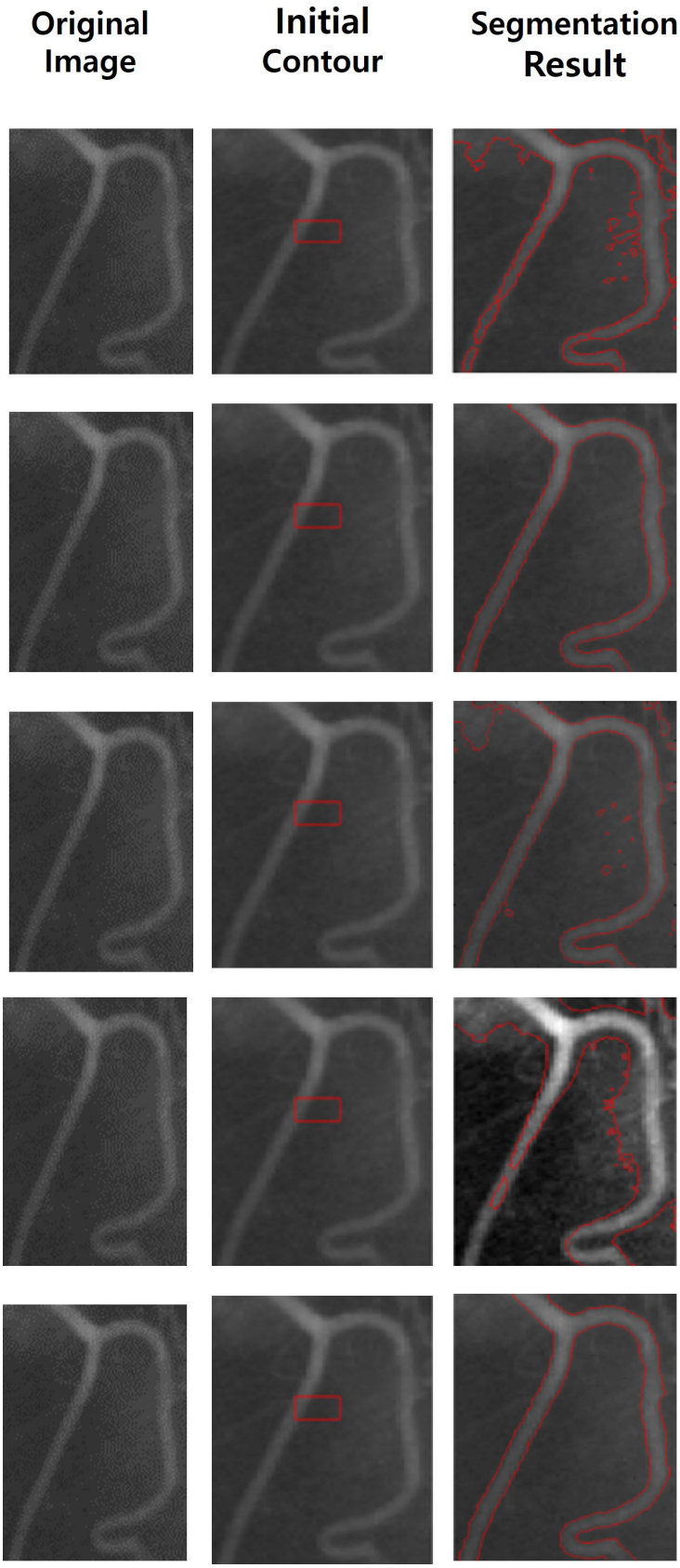

FIGURE 6. Segmentation results of various models including the proposed method: (Top Row) CV, (Second Row) LIF, (Third Row) GLFIF, (Fourth Row) HLFRA, (Fifth Row) proposed model.

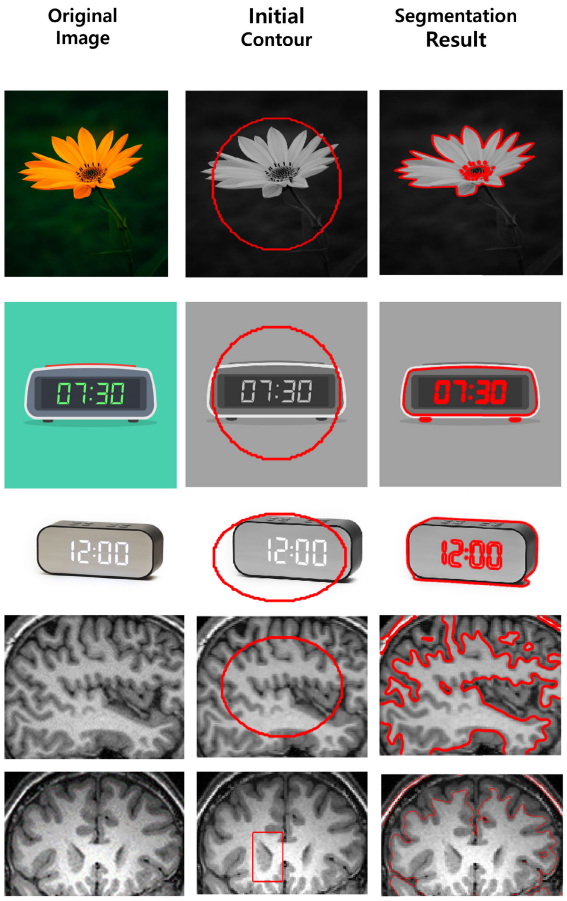

FIGURE 7. A series of images is presented, showcasing the results achieved by the proposed model.

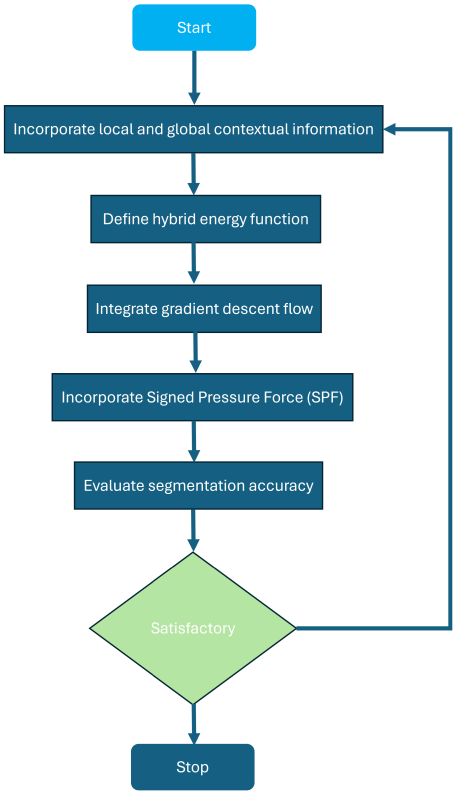

FIGURE 8. Graphical abstract illustrating the proposed model.

V. CONCLUSION

In this research, we introduced a novel image segmentation model based on active contour techniques, addressing limitations of prior methods and achieving significant progress in the field. Our model consistently delivered precise and efficient segmentation results, even in scenarios with intensity inhomogeneity, weak edges, and noisy images, as demonstrated through comprehensive analysis and evaluation.

Our model's superiority became evident when evaluated on diverse intensity inhomogeneous data. It excelled in segmenting challenging objects with black borders, a task where many conventional methods struggle. Leveraging level sets and energy functions, our model adeptly handled complex boundaries, resulting in more accurate segmentations.

Furthermore, our approach exhibited resilience and efficiency when dealing with weak edges and inhomogeneous images. With reduced sensitivity in initial contour placement and faster convergence, our model outperformed other techniques like WHRSPF and DRLSE. It also significantly reduced computational time, emphasizing its practicality for real-world applications.

Quantitative comparisons validated our model's performance with metrics like Accuracy, Dice Index, and Sensitivity. Close alignment between detected areas and ground truth underscored the precision of our segmentation results.

Our proposed image segmentation methodology represents a substantial advancement, offering heightened precision, efficiency, and adaptability. Its ability to accommodate various intensity distributions and complex boundaries positions it as a valuable tool across diverse applications, including medical imaging and computer vision.

Our study contributes to the evolution of image segmentation approaches, opening new possibilities for image analysis across multiple industries.

REFERENCES

[1] A. Tsai, A. Yezzi, and A. S. Willsky, "Curve evolution implementation of the mumford-shah functional for image segmentation, denoising, interpolation, and magnification," *IEEE Trans. Image Process.*, vol. 10, no. 8, pp. 1169–1186, Aug. 2001.

[2] C. Li, C.-Y. Kao, J. C. Gore, and Z. Ding, "Implicit active contours driven by local binary fitting energy," in *Proc. IEEE Conf. Comput. Vis. Pattern Recognit.*, Jun. 2007, pp. 1–7.

[3] T. F. Chan and L. A. Vese, "Active contours without edges," *IEEE Trans. Image Process.*, vol. 10, no. 2, pp. 266–277, Feb. 2001.

[4] K. Ding, L. Xiao, and G. Weng, "Active contours driven by region-scalable fitting and optimized Laplacian of Gaussian energy for image segmentation," *Signal Process.*, vol. 134, pp. 224–233, May 2017.

[5] K. Zhang, H. Song, and L. Zhang, "Active contours driven by local image fitting energy," *Pattern Recognit.*, vol. 43, no. 4, pp. 1199–1206, Apr. 2010.

[6] C. Li, R. Huang, Z. Ding, J. C. Gatenby, D. N. Metaxas, and J. C. Gore, "A level set method for image segmentation in the presence of intensity inhomogeneities with application to MRI," *IEEE Trans. Image Process.*, vol. 20, no. 7, pp. 2007–2016, Jul. 2011.

[7] J. Fang, H. Liu, J. Liu, H. Zhou, L. Zhang, and H. Liu, "Fuzzy region-based active contour driven by global and local fitting energy for image segmentation," *Appl. Soft Comput.*, vol. 100, Mar. 2021, Art. no. 106982.

[8] J. Fang, H. Liu, L. Zhang, J. Liu, and H. Liu, "Region-edge-based active contours driven by hybrid and local fuzzy region-based energy for image segmentation," *Inf. Sci.*, vol. 546, pp. 397–419, Feb. 2021.

[9] H. Ali, N. Badshah, K. Chen, and G. A. Khan, "A variational model with hybrid images data fitting energies for segmentation of images with intensity inhomogeneity," *Pattern Recognit.*, vol. 51, pp. 27–42, Mar. 2016.

[10] H. Liu, Y. Chen, W. Chen, "Neighborhood aided implicit active contours," in *Proc. IEEE Conf. Comput. Vis. Pattern Recognit.*, vol. 1, Jun. 2006, pp. 841–848.

[11] R. Ronfard, "Region-based strategies for active contour models," *Int. J. Comput. Vis.*, vol. 13, no. 2, pp. 229–251, Oct. 1994.

[12] L. Wang, C. Li, Q. Sun, D. Xia, and C.-Y. Kao, "Active contours driven by local and global intensity fitting energy with application to brain MR image segmentation," *Computerized Med. Imag. Graph.*, vol. 33, no. 7, pp. 520–531, Oct. 2009.

[13] K. Zhang, Q. Liu, H. Song, and X. Li, "A variational approach to simultaneous image segmentation and bias correction," *IEEE Trans. Cybern.*, vol. 45, no. 8, pp. 1426–1437, Aug. 2015.

[14] C. Li, C.-Y. Kao, J. C. Gore, and Z. Ding, "Implicit active contours driven by local binary fitting energy," in *Proc. IEEE Conf. Comput. Vis. Pattern Recognit.*, Jun. 2007, pp. 1–7.

[15] K. Ding, L. Xiao, and G. Weng, "Active contours driven by local pre-fitting energy for fast image segmentation," *Pattern Recognit. Lett.*, vol. 104, pp. 29–36, Mar. 2018.

[16] C. Li, C.-Y. Kao, J. C. Gore, and Z. Ding, "Implicit active contours driven by local binary fitting energy," in *Proc. IEEE Conf. Comput. Vis. Pattern Recognit.*, Jun. 2007, pp. 1–7.

[17] J. Fang, H. Liu, L. Zhang, J. Liu, and H. Liu, "Active contour driven by weighted hybrid signed pressure force for image segmentation," *IEEE Access*, vol. 7, pp. 97492–97504, 2019, doi: 10.1109/ACCESS.2019.2929659.

[18] X. Liu, Y.-M. Cheung, M. Li, and H. Liu, "A lip contour extraction method using localized active contour model with automatic parameter selection," in *Proc. 20th Int. Conf. Pattern Recognit.*, Aug. 2010, pp. 4332–4335.

[19] M. Kass, A. Witkin, and D. Terzopoulos, "Snakes: Active contour models," *Int. J. Comput. Vis.*, vol. 1, no. 4, pp. 321–331, Jan. 1988.

[20] A. Niaz, K. Rana, A. Joshi, A. Munir, D. D. Kim, H. C. Song, and K. N. Choi, "Hybrid active contour based on local and global statistics parameterized by weight coefficients for inhomogeneous image segmentation," *IEEE Access*, vol. 8, pp. 57348–57362, 2020.

[21] C. Li, C.-Y. Kao, J. C. Gore, and Z. Ding, "Implicit active contours driven by local binary fitting energy," in *Proc. IEEE Conf. Comput. Vis. Pattern Recognit.*, Jun. 2007, pp. 1–7.

[22] C. Li, C.-Y. Kao, J. C. Gore, and Z. Ding, "Implicit active contours driven by local binary fitting energy," in *Proc. IEEE Conf. Comput. Vis. Pattern Recognit.*, Jun. 2007, pp. 1–7.

[23] C. Li, R. Huang, Z. Ding, C. Gatenby, D. Metaxas, and J. Gore, "A variational level set approach to segmentation and bias correction of images with intensity inhomogeneity," in *Proc. Int. Conf. Med. Image Comput. Comput.-Assist. Intervent.* Berlin, Germany: Springer, 2008, pp. 1083–1091.

[24] (2003). *The Mini-MIAS Database of Mammograms*. [Online]. Available: http://peipa.essex.ac.uk/info/mias.html

[25] Y. Yu, C. Zhang, Y. Wei, and X. Li, "Active contour method combining local fitting energy and global fitting energy dynamically," in *Proc. Int. Conf. Med. Biometrics*. Berlin, Germany: Springer, 2010, pp. 163–172.

[26] A. Tiwari, S. Srivastava, and M. Pant, "Brain tumor segmentation and classification from magnetic resonance images: Review of selected methods from 2014 to 2019," *Pattern Recognit. Lett.*, vol. 131, pp. 244–260, Mar. 2020.

[27] J. Fang, H. Liu, L. Zhang, J. Liu, and H. Liu, "Fuzzy region-based active contours driven by weighting global and local fitting energy," *IEEE Access*, vol. 7, pp. 184518–184536, 2019.

[28] C.-Y. Yu, W.-S. Zhang, Y.-Y. Yu, and Y. Li, "A novel active contour model for image segmentation using distance regularization term," *Comput. Math. Appl.*, vol. 65, no. 11, pp. 1746–1759, Jul. 2013.

[29] A. Niaz, E. Iqbal, F. Akram, J. Kim, and K. N. Choi, "Self-initialized active contours for microscopic cell image segmentation," *Sci. Rep.*, vol. 12, no. 1, p. 14947, Sep. 2022.

[30] E. Elkhateeb, H. Soliman, A. Atwan, M. Elmogy, K.-S. Kwak, and N. Mekky, "A novel coarse-to-fine sea-land segmentation technique based on superpixel fuzzy C-means clustering and modified chan-vese model," *IEEE Access*, vol. 9, pp. 53902–53919, 2021, doi: 10.1109/ACCESS.2021.3065246.

[31] E. Iqbal, A. Niaz, A. A. Memon, U. Asim, and K. N. Choi, "Saliency-driven active contour model for image segmentation," *IEEE Access*, vol. 8, pp. 208978–208991, 2020, doi: 10.1109/ACCESS.2020.3038945.

[32] Q. Cai, H. Liu, Y. Qian, J. Li, X. Duan, and Y.-H. Yang, "Local and global active contour model for image segmentation with intensity inhomogeneity," *IEEE Access*, vol. 6, pp. 54224–54240, 2018, doi: 10.1109/ACCESS.2018.2871846.

[33] H. Liu, J. Fang, Z. Zhang, and Y. Lin, "A novel active contour model guided by global and local signed energy-based pressure force," *IEEE Access*, vol. 8, pp. 59412–59426, 2020, doi: 10.1109/ACCESS.2020.2981596.

[34] X. Yang, X. Jiang, L. Zhou, Y. Wang, and Y. Zhang, "Active contours driven by local and global region-based information for image segmentation," *IEEE Access*, vol. 8, pp. 6460–6470, 2020, doi: 10.1109/ACCESS.2019.2963435.

[35] A. Niaz, A. A. Memon, K. Rana, A. Joshi, S. Soomro, J. S. Kang, and K. N. Choi, "Inhomogeneous image segmentation using hybrid active contours model with application to breast tumor detection," *IEEE Access*, vol. 8, pp. 186851–186861, 2020.

[36] A. Niaz, E. Iqbal, A. A. Memon, A. Munir, J. Kim, and K. N. Choi, "Edge-based local and global energy active contour model driven by signed pressure force for image segmentation," *IEEE Trans. Instrum. Meas.*, vol. 72, 2023, Art. no. 5033014.

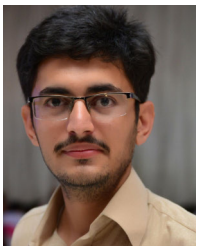

HAMZA ZIA received the B.S. degree in computer science from Comsats University Islamabad, in 2021. He is currently pursuing the master's degree in computer science with Chung-Ang University, Seoul, South Korea. His research interests include anomaly detection, image segmentation, and object detection.

SHAFIULLAH SOOMRO received the Bachelor of Engineering (B.E.) degree from QUEST, Nawabshah, Sindh, Pakistan, in 2008, the Master of Engineering (M.E.) degree from MUET, Jamshoro, Sindh, in 2014, and the Ph.D. degree in computer science from Chung-Ang University, Seoul, South Korea, in 2018. He is currently a Postdoctoral Researcher with the Department of Computer Science and Media Technology, Linnaeus University, Sweden. His research interests include motion tracking, object segmentation, and 3D image recognition.

KWANG NAM CHOI received the B.S. and M.S. degrees from the Department of Computer Science, Chung-Ang University, Seoul, South Korea, in 1988 and 1990, respectively, and the Ph.D. degree in computer science from the University of York, U.K., in 2002. He is currently a Professor with the School of Computer Science and Engineering, Chung-Ang University. His current research interests include motion tracking, object categorization, and 3D image recognition.